A DECOMPOSITION TECHNIQUE FOR IMAGE FUSION TO DETECT BRAIN TUMOR USING T1, T2 WEIGHTED MR IMAGES

Padmanjali. A. Hagargi[1], Dr. Shubhangi. D. C[2]
[1]Asst Prof. Ise Dept, Gndec, Bidar
[2]Prof. Hod Cse Dept, Vtu Pg Centre Kalburgi

Abstract
A technique in imaging that is used to detect the brain tumor is magnetic resonance imaging (MRI). One of the most dangerous diseases occurring among adults and also in children's is a brain tumor. As there is an advancement in medical science , with this paper an opportunity in survival of patients is approached if tumor is identified in the early stage, an automatic approach to image classification is an emerging research area in the medical field. Here the proposed method is presented an efficient tumor detection and its classification approach using efficient fusion techniques and segmentation algorithms. In the proposed system pre-processing block includes wiener filtering that removes the noisy pixels from the image. The proposed method uses fusion of T1 and T2 slices of MRI image for efficient tumor detection. By using techniques like QT decomposition for Image fusion, Level Set Segmentation to detect the tumor region, feature extraction techniques like GLCM, Gray Level Run Length Matrix (GLRLM). Along with ANN classifier for classification, the proposed method shows an average accuracy of about 93.97.

Keywords: QT Decomposition, Level Set Segmentation, T1,T2 weighted MRI, ANN, Wiener Filter

I. INTRODUCTION

The tumor in Brain is nothing but a group of abnormal cells they grow around or within the brain. The tumor is a large mass of tissues; they grow out of control of the normal forces that controls the growth. Tumors have the capability to destroy all the cells which are healthy. The tumor can also damage indirectly the existing healthy cells by joining other parts of the brain and causing inflammation, brain swelling and pressure inside the skull. Over the last twenty years, the overall incidence of cancer, including brain cancer, has increased by more than10%, as reported in the National Cancer Institute statistics (NCIS). The National Brain Tumor Foundation (NBTF) is the research center in the U.S gives the estimation of about 29,000 people in the U.S are identified with suffering from primary brain tumors every year and about 13,000 people are found dying. The overall yearly incidents of the initial brain tumors in the U.S is about 12 to 12 for primary malignant tumors, that rate is about 6 to 7 people per 1,00,000 people.

About 17 out of every 1,010 cancers diagnosed in the U.K are in the brain (or 1.6%). In India, more than 80,271 persons are affected with various types of tumor.

The modality of imaging produces images of soft tissue. The captured medical images show the internal structure, but the doctors want more than the peer images to depict the informations like finding abnormal tissue, shape and so on. If such observations are covered by the doctors themselves, chances to be inaccurate are more and are very time-consuming. Hence using an efficient segmentation is necessary to get an accurate result by detecting and extracting tumor region in MRI images.

Usually, there are 2 types of the tumor: Benign; Malignant. The tumor which doesn't expand in an abrupt way is a benign type of tumor. It does not affect the neighboring tissues which are healthy. A malignant tumor is the type of tumor that grows with the passage of time and worsens the situation leading to death. This disease is a severe progressing disease. This disease leads to cancer usually. Hence enormous research has been carried in the recent years for the efficient segmentation and the tumor classification in the given MRI of the Tumor in the brain.

In our proposed method, the pictorial information of 2 slices of MRI imaging; T1 and T2 are integrated that will provide the extended information about the brain internal structuring. Based on this information tumor sections are segmented from the image by making use of the level set segmentation. The necessity for classification of segmented images into the tumor or non-tumor sections is provided by feature vectors. Features are accumulated by decomposing images using RPCA and Quadtree, and then building features using GLCM, GLRLM, PHOG and CLBP methods. Classification is dependent on these feature vectors and ANN classifier has finally made efficient tumor classification into benign and malignant.

II. LITERATURE SURVEY

Mohammad Havaei et.al [01] presented a fully automatic brain tumor segmentation approach using DNNs (Deep Neural Networks). This work considered both high and low-grade pictures in MRI. Proposed CNN in this work exploits both the local features and the contextual global features simultaneously. The evaluation of the algorithm is done on the BRATS test dataset.

Bjoern H. Menze et.al [02] reported the set up along with results of BRATS (Multimodal Brain Tumor Image Segmentation Benchmark). Fusing of several algorithms which are good using a hierarchical segmentation approach based on majority yielded Vote that ranked consistently above all the individual algorithm is done.

Nelly Gordillo et.al [03] presents an overview of more relevant segmentation of the brain tumor methods that are conducted after the image acquisition. This paper reviewed main approaches of the automated MS segmentation of lesion. A qualitative and quantitative comparison of results of approaches analyzed is also presented.

El-Sayed Ahmed El-Dahshan et.al [06] presented the hybrid technique to classify the MRI. In this paper classification process, development of two classifiers is done. The 1st classifier is based on the feed-forward back propagation artificial neural network (FP-ANN) and the 2nd classifier is based on the k nearest neighbor (k-NN). The classifiers are used to classify the subjects as the abnormal or normal MRI human images.

Manavalan Radhakrishnan et.al [10] proposed work for TRUS prostate images. Statistical parameters are calculated for analysis of classifier performance such as; sensitivity, specificity, and accuracy. The comparison of features sets is done here by examining the individual based features results and combined feature results. Histogram and GLRLM features are giving poor performance and histogram, GLRLM and GLCM combined features stood well for the classification. Researchers in [11], [12], [13], [14], [15], [16], [17], [18], [19], [20], [21], [22], [23], [24], [25] are also proposed an efficient techniques for tumor detection. In the proposed methodology for efficient tumor detection in the entire input query MRI images using efficient techniques like RPCA and QT decomposition for Image fusion, Level Set Segmentation to detect the tumor region, feature extraction techniques like GLCM and Gray-Level Run-Length Matrix (GLRLM) Along with ANN classifier for classification of final result on tumor or non-tumor.

III. METHODOLOGY

Preprocessing and Fuzzy based Image Fusion using Quadtree Decomposition

It consists of two phases called Testing phase and the Training Phase. In the testing phase initially the input MRI images T1, T2 are passed to the Pre-processing block. In pre-processing, different pre-processing steps like Resizing, RGB to Grayscale conversion and the noise removal also done. Resizing step includes changing size of input to some fixed size. In the Noise Removal step noise removal using the filter called Wiener is made use. Once the T1 and T2 images are filtered both the images are passed to Image Fusion Block. In the Fusion block, both these images are then decomposed to get the fused image using QT decomposition.

The obtained fused image then passed to Feature Extraction block. A technique like Level Set Segmentation is used to detect the tumor region. The segmented region may contain a tumor or non-tumor region, hence extracting the appropriate features from it is very necessary to find the exact tumor region. Prominent features from these segmented regions are extracted using GLCM and GLRLM techniques. The Extracted features then passed to ANN classifier. In training phase segmented tumor image samples taken as the input and are passed to pre-processing block to follow the same steps as carried in the testing phase. Features from these samples are extracted and are stored in the knowledge base. Every time during the classification the extracted features from the Query image is compared with the features already stored in the Knowledgebase to classify if the Query image contains disease or not.

Entire framework of this Fuzzy based image fusion is as shown in the Fig.1. It is proven that the RPCA is to be one of the effective techniques to recover both spare and low-rank components from the data of high dimension. In this approach a data input matrix $\mathrm{D} \in \mathrm{i}^{\mathrm{M}\times\mathrm{N}}$ is made to subject itself to low-rank property. To regain the structure of low-rank, D can be decomposed as given below,

$$\mathrm{D} = \mathrm{A} + \mathrm{E}, \qquad \mathrm{rank}(\mathrm{A}) = \min(\mathrm{M}, \mathrm{N}) \qquad (1)$$

Where principle matrix is represented by matrix A and spare matrix is represented by matrix E. Hence to overcome this difficult task a demonstration is done saying that w.r.t the rank of A and also when the spare matrix E is sufficiently spare, accurate recovery of the Matrix A from D is done only on solving the optimized problem given below,

$$\min_{(\mathrm{A},\mathrm{E})} \|\mathrm{A}\|_* + \lambda\|\mathrm{E}\|_1 \quad \mathrm{s.t.} \ \ \mathrm{A} + \mathrm{E} = \mathrm{D} \qquad (2)$$

Where $\|\cdot\|_*$ depicts the nuclear norm of the principle matrix A, $\|\cdot\|_1$represents the l_1 the norm of the spare matrix E and positive weighting parameter is denoted by λ.

Fig. 1: Block Diagram for Fusion using RPCA and Quadtree Decomposition

In the QuadTree Decomposition (QT) structure, each one of these internal nodes has four partitions and these leaf nodes present in the tree has no partition. This analysis technique always partitions image into blocks. These blocks are comparatively more homogeneous to the image itself. In the traditional technique of QT decomposition, a sized image is always divided into parts of four equal sized blocks and these blocks are checked with some threshold conditions of homogeneity regions. If the divided block reaches the threshold condition then it is not divided further, blocks which will not meet this criterion is divided further into four blocks. This step is continued till the blocks meet the threshold condition. Processing of this decomposition, division approach is first performed on the image with low resolution and then on the image with high resolution based on the low-resolution image division. This approach is chosen for its self-adaption and high-speed property. This approach also eliminated artifacts involved in the fused image.

The proposed technique for fusion approach is as shown in the Fig.1. In the proposed approach of fusion, a novel method of fusion is carried out. An optimal approach of subdivision is obtained using an efficient QT decomposition technique. As in the flow given below, two source images Image-1 and Image-2 is taken and are presumed to be preregistered before passing as the input.

Matrix D as explained above using RPCA decomposition approach is constructed. Once the decomposition is done principle matrix A and spare matrix E is obtained. Based on the salient homogeneity region of the matrix E the better partition of Matrix E always corresponds to the improved partition of the spare matrix. The temporary fusion spare matrix is constructed by averaging the two matrices. Next step is partitioning the temporary spare matrix into a number of blocks using QT decomposition. Based on the results obtained, this matrix is splited into two spare matrices. As described above if the region homogeneity of the block does not meet the defined threshold conditions they are terminated for further QT decomposition. Next step is to calculate the sharpness as in the eq. (3) below, where E_{m1} and E_{m2} are the spare matrix blocks obtained. $\mathrm{E}_{\mathrm{m1}}^{(\mathrm{k})}$ And $\mathrm{E}_{\mathrm{m2}}^{(\mathrm{k})}$ denote the kth blocks of sparse matrices E_{m1} and E_{m2} respectively. $\mathrm{EOG}_{\mathrm{k}}^{\mathrm{E_A}}$ Denotes the EOG-Energy of image gradient and $\mathrm{EOG}_{\mathrm{k}}^{\mathrm{E_B}}$ be the EOG of $\mathrm{E}_{\mathrm{m1}}^{(\mathrm{k})}$ and $\mathrm{E}_{\mathrm{m2}}^{(\mathrm{k})}$, accordingly. EOG of each sparse matrix block can be defined as,

$$\begin{cases} \mathrm{EOG} = \sum_i \sum_j (E_i^2 + E_j^2) \\ E_i = E(i+1, j) - E(i, j) \\ E_j = E(i, j+1) - E(i, j) \end{cases} \quad (3)$$

Where $E(i, j)$ represents the value of the element at the position (i, j) in sparse matrix block. Followed by creating decision matrix using the eq. (4) is done. Where "1" in H depicts the pixel at position (i, j) in the input Image-1 becomes clearer, and while "0" in H represents the pixel at position (i, j) in the input Image-2 becomes clearer [26]. The final fused image is obtained using the fusion rule given in the eq. (5).

$$H(i, j) = \begin{cases} 1, & \mathrm{EOG}_k^{E_A} \geq \mathrm{EOG}_k^{E_B} \\ 0, & \text{otherwise} \end{cases} \quad (4)$$

$$F(i, j) = \begin{cases} \mathrm{Image1}(i, j), & H(i, j) = 1 \\ \mathrm{Image2}(i, j), & H(i, j) = 0 \end{cases} \quad (5)$$

Once the final fused image is obtained they are again compared with certain fuzzy rules. Usually, fuzzy machines will always work on certain fuzzy sets for decision making to perform better fusion. The QT decomposition used in our research work is a decomposing image with 6 iterations, for the image of dimensions 256 X 256, here the dimensions include a number of rows and column number. For the QT decomposition of two images T1 and T2 all the pixels are concatenated into one vector form of size 65536.

3.1 Level Set Segmentation

The level set approach is one of the emerging image segmentation approaches for the segmentation of the medical images. This approach is important in tracking shapes and interfaces. The basic idea behind this approach is to represent contours as the level set of zero of an implicit function defined in high dimension, which is usually referred as level set function.

Level set segmentation method can be formulated with strong mathematical theories as fallows, Initially starts with setting of segmentation boundaries in which the contour level must be at zero level, for this the implicit surface is given as,

$$\emptyset(X, t) = \mp d \quad (6)$$

Where = Implicit Surface, X= Position of taken image, t = Time, d= Distance between X and the zero level set. 'd' values vary as positive or negative, the condition behind this is, if 'X' position is outside zero level set then 'd' is positive or else 'd' is negative [27].

By tracking and interfacing the level zero set $\tau(t)$ it will be very much easy to approximate the active contours evaluation which is directly dependent on PDE function$\emptyset(t, x, y)$. Implicit interface of zero level set is given by

$$\tau(t) = \begin{cases} \emptyset(t, x, y) < 0 & (x, y) \text{ is inside } \tau(t) \\ \emptyset(t, x, y) = 0 & (x, y) \text{ is at } \tau(t) \\ \emptyset(t, x, y) > 0 & (x, y) \text{is outside } \tau(t) \end{cases} \quad (7)$$

By knowing the level set function values it is pretty much easy to estimate the topological changes of the implicit interface ' ', numerical equation for level set with evolution of ' " is given by,

$$\begin{cases} \dfrac{\partial \emptyset}{\partial t} + F|\nabla \emptyset| = 0 \\ \emptyset(0, x, y) = \emptyset_0(x, y) \end{cases} \quad (8)$$

Where $|\nabla \emptyset|$= Normal directionType equation here.

$\emptyset_0(x, y)$= Contour at initial levels

F= Internal and external forces

By using the edge indication function 'h' the forces can be normalized in order to block the level set evolution along with the optimal solution,

$$h = \frac{1}{1 + |\nabla(G_\sigma * I)^2|} \quad (9)$$

Where G_σ represents the Gaussian kernel and I is the considered image. Level set segmentation standard formula with all the parameters which are explained above is given as

$$\frac{\partial \emptyset}{\partial t} = h|\nabla \emptyset| \left(\mathrm{div} \left(\frac{\nabla \emptyset}{|\nabla \emptyset|} \right) + v \right) \quad (10)$$

The computation time for all the steps and mathematical theories as very high in order to overcome these drawbacks and also to get the better output the fuzzy clustering technique is combined with the level set segmentation technique to form one hybrid technique called spatial fuzzy clustering algorithm, which is explained in the previous section. For the proposed research work 256 X 256 dimensional passing of images to level set segmentation that segments image with iterations of 198.

3.2 Feature Extraction

Quantifiable property of an object is specified by each of these features and only significant information's are later picked from these features. Features are classified into different types which are general features and Global features. The features which are independent based on the application are called General features. The features which are obtained during the edge detection by considering the subdivision of the bands of the image and segmentation of the image then it is called as local features. The two features used in this work is grey-level co-occurrence matrix (GLCM) and grey-level run-length matrix (GLRLM). In our work 128X128 image dimension is passed to GLCM, this will calculate approximately 22 features for the query image. Total features calculated by GLCM are 1 X 44 vectors. Similarly, GLRLM is generating features of number 7 i.e.1 X 7 vector. So the total number of features developed by both techniques is 1 X 51 vectors.

3.3 Grey-Level Co-Occurrence Matrix

Depending on the pixel number in each of the combination, first order statistics, second order statistics or higher order statistics are considered. Based on the GLCM the second order statistics is used to analyze the image as a texture. GLCM approach is the tabulation of the frequency or how often a combo of pixel brightness values in an image occurs. The Fig. 2 given below represents the GLCM formulation of the gray level of four levels in an image of distance d = 1 and the 0° direction.

Fig. 3 (a) depicts the example matrix of the pixel intensity which represents the image with four levels of gray. The intensity level 1 and 0 are marked within a thin box. The thin box represents the pixel intensity 0 with the pixel intensity 1 as its neighbor. There are usually two occurrences of pixels of such types. Hence the matrix of GLCM is formed as in Fig. 1(b) with value two in 0 rows, column 1. Similarly, GLCM matrix column 0 and row 0 is also has been given a value of two, because of occurrences of two in which the pixel with the value 0 has 0 pixels as its neighbor in the horizontal direction. Due to which the pixels matrix in (a) can be transformed into a GLCM as (b). Not only to the horizontal direction, GLCM can also be formed in different directions like 90 º, 45 ºand 135 º as depicted 'i' the Fig. 2 [28].

0	0	1	1	1
0	0	1	1	1
0	2	2	2	2
2	2	3	3	3
2	2	3	3	3

(a)

	0	1	2	3
0	2	2	1	0
1	0	4	0	0
2	0	0	5	2
3	0	0	0	4

(b)

Fig. 1: (a) Example Matrix of the Pixel Intensity; (b) GLCM Matrix

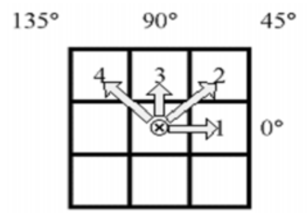

Fig.2: Different Directions Formed by GLCM

From centre to the 1st pixel representing direction = 0° with distance 'd' =1, to the pixel 2 direction = 45° with the distance d = 1 and also to the 3rd pixel direction = 90° with distance d = 1, and to the pixel 4 direction = 135° with distance d = 1. Even though the co-occurrence matrices extract the properties of texture, it is not directly used an analysis tool. The matrix of this is again extracted to fetch the numbers that are usually used for texture classification. The above created GLCM matrix is then applied to segmented regions. Mathematically, for a given image I of size $\mathrm{K} \times \mathrm{K}$ (256×256), the elements of a $\mathrm{G} \times \mathrm{G}$ $(8 \times 8 \times 4)$ gray-level co-occurrence matrix MCO for a displacement vector $\mathrm{d} = (\mathrm{dx}, \mathrm{dy})$ is defined as in eq. (11). The defined value 'd' for angle 0 is [0 d], for angle 45 is [-d d], angle for 90 is [-d 0] and for degree 135 is [-d d].

$$M_{co} = \sum_{x=1}^{k}\sum_{y=1}^{k}\begin{cases}1, \text{if } I(x,y) = i \text{ and } I(x+d_x, y+d_y) = j \\ 0\end{cases} \quad (11)$$

In the proposed work four important features like contrast, energy, entropy, and Correlation are extracted. Contrast calculates the intensity level difference between the adjacent pixels in a considered image and is given as fallows by the equation below,

$$\mathrm{Contrast} = \sum_{i,j} |i-j|^2 p(i,j) \quad (12)$$

Where $p(i,j)$ denotes the position of the GLCM in that the value represents the sum of co-occurrence between adjacent pixels of i and its neighbor j. Correlation measures the level of correlations between pixels against the remaining pixels in the Input image. Also, Correlation computation finds the linear dependency levels of gray of the neighboring pixels and is it is given by,

$$\text{Correlation} = \sum_{i,j} \frac{(i-\mu_i)(j-\mu_j)p(i,j)}{\sigma_i \sigma_j} \qquad (13)$$

The energy measures the summation of the squared element in the entire GLCM. It is denoted by the eq. (15),

$$\text{Energy} = \sum_{i,j} p(i,j)^2 \qquad (14)$$

Information which compress the considered image and it contains the loss of information from the image for GLCM calculation is referred as entropy and it is given as,

$$\text{Entropy} = \sum_{i=0}^{N_g-1} \sum_{j=0}^{N_g-1} -p_{ij} * \log p_{ij} \qquad (15)$$

The formulation and extraction of the input NPK segments are extracted using MATLAB for calculating GLCM to get feature vector.

3.4 Gray-Level Run-Length Matrix (GLRLM)

GLRLM is nothing but a matrix from which the texture features is extracted for the analysis of texture. Usually this texture is called as the grey intensity pixel of pattern in a particular direction from the reference pixel. Run Length is defined as the pixel number that is adjacent having the same intensity of grey in the particular direction.

1	2	3	4
1	3	4	4
3	2	2	2
4	1	4	1

(b)

Gray Level	Run Length(j)			
	1	2	3	4
1	4	0	0	0
2	1	0	1	0
3	3	0	0	0
4	3	1	0	0

(b)

Fig.3: (a) Matrix with 4 Different Gray Levels; (b) Values for Run Length

GLRLM is usually a two dimensional matrix, where each of the element $p(i,j|\theta)$ is the number of elements j with the intensity value i present in the direction . Fig.4: depicts the matrix with 4 different gray levels.

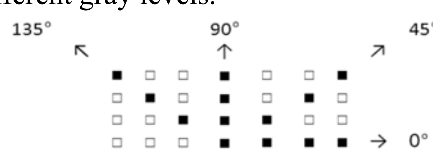

Fig. 4: Directions of GLRLM Matrix

These matrices represent the GLRL matrix in the direction 0° $(p(i,j|\theta)$, In addition with the 0°, GLRLM matrix can also be represented in the other direction i.e. 90 º, 45 ºand 135 º as depicted in the Fig.4. Some of the texture features extracted from GLRLM are: SRE (Shot Runs Emphasis), GLN (Gray Level Non-uniformity), LRE (Long Run Emphasis), RP (Run Percentage) and RLN (Run Length Non-uniformity) was identified.

3.5 Back Propagation Neural Network (BPNN)

Transmission of signals in synapses from one of the neuron is done to generate these chemical processes. To lower or raise electrical potential within body of the receiving cell this effect is utilised. The cell is fired if the potential exceeds the threshold. Here the ANN (Artificial neural networks) is as developed as generalizations for the mathematical items of the biological nervous systems. Transfer function represents the nonlinear characteristics exhibited by neurons. The detailed architecture of neural network is explained briefly below [29], [30].

Classifier will initiate the classification by defining architecture for network. This includes the neurons network number and layers in the network. Once based on the collected features network is created it intakes the features for training Data. The trained features are compared with the current features of query image. If the satisfactory level is achieved for the particular feature output layer is updated if not then loop will be continued until the query image are matched with any one section of trained data. Dig. 5: gives tree likenetwork to understand about ANN and Fig. 6: gives the algorithmic steps of ANN.

ANN architecture mainly consists of 3 types of the neuron layers called input layer, hidden and output layer. In feed forward kind of networks signal flow is mainly from the input to output units. Exactly in the feed forward direction. The processing of data can extended over multiple layers of units with the absence of feedback connections. Feedback connections are present in recurrent networks.

There are 3 different sorts of learning situations: reinforcement learning, Supervised and non supervised learning. In the supervised learning approach input vector along with desired responses are represented at the input. Forward pass and the error calculation between the actual and desired response are also done.

- Perceptron Learning

The perceptron is another form of neural network in which the weights and the bias are trained to produce a correct target vector. The Technique used here for learning is called perceptron learning. Perceptrons are suited for simple problems in pattern classification.

- Back propagation Learning

This tells us that the error is increasing when the weight is increasing. And hence adding negative value to the weight is an obvious thing and vice versa if in case of negative derivative.

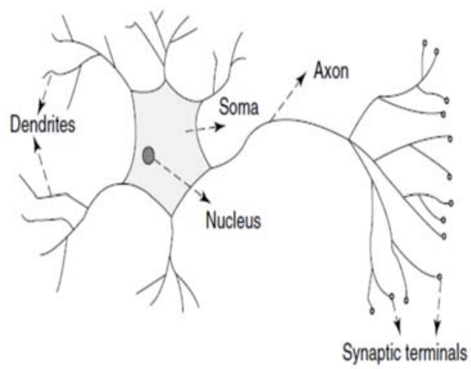

Fig.5:Treelike Networks of the Nerve Fibers in ANN

Algorithm 1: Back Propagation Neural Network

Input: weights of segmented Image
Output: classified tumor section
Step1: Choose initial weights randomly w_i
Step2: While Error is too large
Step3: For loop Consider training pattern present in the random order
Step4: Apply the inputs
Step5: For every neuron η calculate output pattern O_p in output layer from input layer, through hidden layer.
Step6: At output layer calculate error.

$$O_{\eta p}\ (\text{Network}) = \frac{1}{1 + e^{-\lambda \text{network}_\eta}}$$

Here, network_η is connection of weights from input to neurons

$$\text{network}_\eta = \text{bias} * w_{\text{bias}} + \sum_k O_{pk}\, w_{k\eta}$$

Step7: pass the error $O_{\eta p}$ (Network) to compute errors for pre-output layer.
Step8: Compute weights using error.
Step9: Apply the weights.
Step10: If Training pattern is < 1
end for
end

Fig.6:ANN Training Module Algorithm

The number of weight updates of the two approaches for the equal number of information shows it is very difficult. The online process weight updates are computed for each and every input data pattern and the weights are modified after each sample. A replacement answer is to compute the weight replaces for each and every input sample, but store these values during one pass by means of the training set which is referred to as an epoch.

At the epoch end, addition of all of the contributions, and weights might be made up to date with the composite value. This process adapts the weights with a cumulative update it is known as the batch-training mode. Training involves feeding the training samples as input vectors through a neural network, error calculation of the output layer and weight adjustment to minimize error in the network. In the research work we are making use of 51 neurons at input layer, 25 neurons at hidden layer and 3 neurons at output layer.

IV. EXPERIMENTAL RESULT

Experiments were conducted on MATLAB R2012a. The collected dataset of 166 MRI images where calcified into tumor and nontumor to train the algorithms and to evaluate the classification and also tumor identification accuracy by cross validation with the ground truth. For each of the MRI images 51 features extracted using GLCM and GLRLM methods. This section depicts the overall results obtained at each stage of the proposed system. Initially the query inputs T1 and T2 slice of the input MRI images as in Fig. 9 a) and (b) is taken and pre-processed to get the noise removed image as in (c) and (d). Next step is to get fused image using techniques like RPCA and QT Decomposition to get the fused image as in (e). Once the fused image is obtained it is necessary for us to predict the exact tumor region. For proper prediction segmentation of the tumor becomes very important. Segmentation is done using the Level set Algorithm.

Level set algorithms undergo 198 iterations to find the tumor regions as in (f) and give the final output as in (g). Output of this stage is then compared with the threshold values to detect the tumor regions as in (h). These segmented regions may be tumor or non tumor, hence to detect the exact tumor feature extraction is done using the techniques like GLCM and GLRLM and is passed to ANN classifier to classify whether it is tumor or non tumor region. The tumor area after classification is as shown in the (i). The validated tumor region is then located in the fused image as in (j). ANN algorithm as shown in fig.8 is the algorithm evaluated on different MRI images consisting of tumor regions. Experiments say that the proposed systems give good results when compared to the existing systems.

Sample image as in Fig.7: (a) and (b) depicts the input image T1 and T2. These images undergo pre-processing steps to get the noise removed images to make it fit for the next stages. These images are later fused to get the fused image. Segmentation of tumor regions in this fused image is done using the level set algorithms. These segments may be tumor or non tumor; hence the validation on this is done using ANN classifier as in (d). The detected tumor is then located in the fused image as in (d).

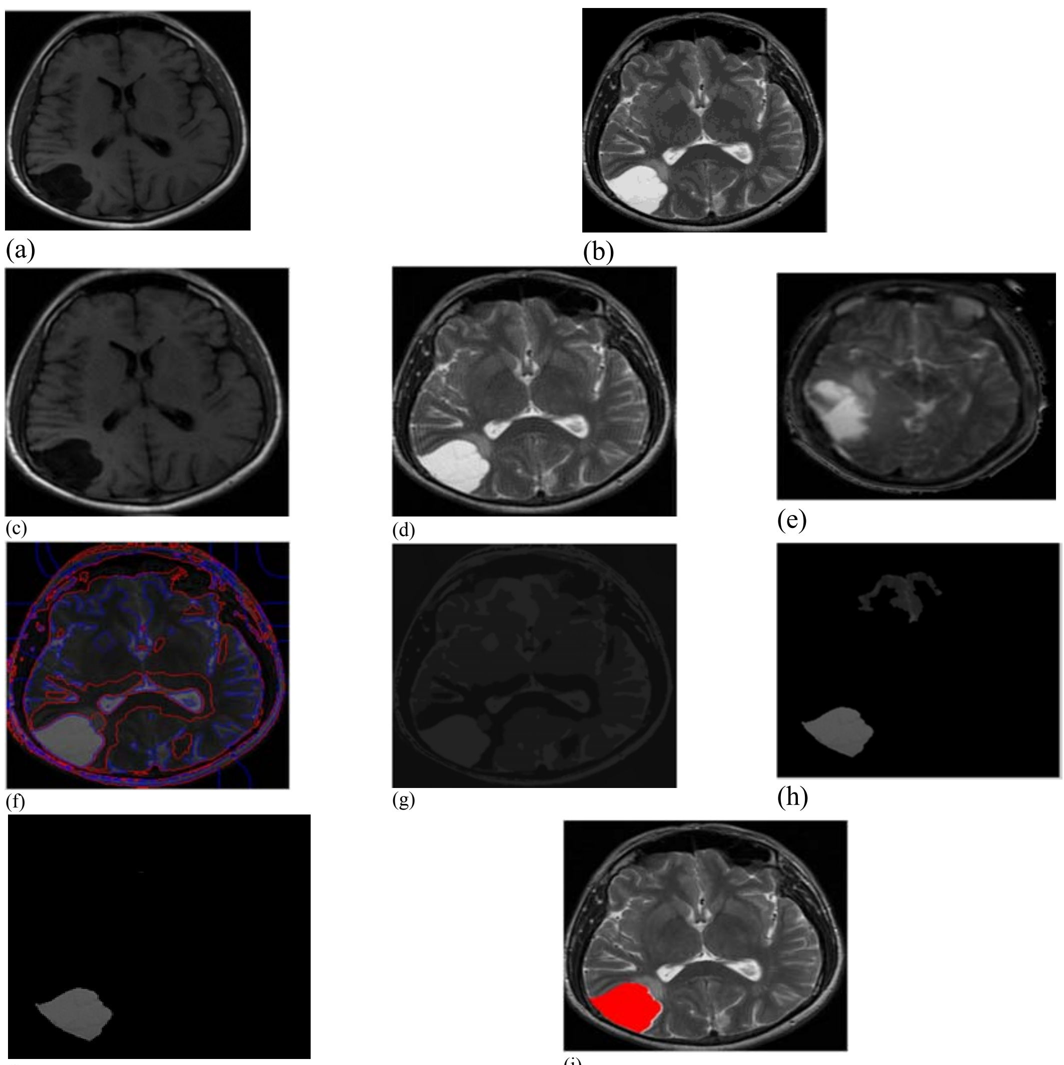

Fig. 7: (a) Input T1 Image; (b) Input T2 Image; (c) Filtered T1 Image; (d) Filtered T2 Image; (e)198 Iterations in the Fused Image; (f) Level Set Segmented Image; (g) Segmented Tumor Parts; (h) Validated Tumor Part; (i) Detected tumor Location in the Fused Image

Similarly various results are obtained by various samples of images as shown in table 2, same process is followed for different samples of images were the Input T1 Image and depicts the Input T2 Image, gives the Segmented Tumor Parts obtained and gives the Validated Tumor Part after classification and finally the Detected tumor Location in the Fused Image.

$$\text{Accuracy} = \frac{\text{TP+TN}}{\text{TP+FP+TN+FN}} \qquad (16)$$

Table 1: Performance Analysis Table for the Proposed System

Dataset	Accuracy
1 (34 images)	94.11
2 (34 images)	94.11
3 (30 images)	93.33
4 (36 images)	94.44
5 (32 images)	93.75
Average (166 images)	93.97

Fig.8: Performance Analysis for various parameters

The fig.8:depicts the proposed methods performance and its comparisons are shown in table1, depicts the comparison for accuracy hparameter with the proposed systems and the existing systems in terms of accuracy and it is found that proposed system gives good results when compared to the existing systems.

Table 1: Comparison Table for Proposed and Existing Systems for Accuracy.

Reference	Methods	Accuracy
An Automatic Brain Tumor Extraction System Using Different Segmentation [31]	Otsu + K-means + Fuzzy-C-Means + Thresholding algorithm	90.57
Analysis of the Brain MRI for Tumor detection & Segmentation [32]	Otsu's segmentation + Overlay based image fusion	93.00
Brain tumor segmentation based on a hybrid clustering technique [33]	K-means Clustering + Fuzzy-C-Means	90.50
Analysis And Evaluation Of Brain Tumor Detection From MRI Using F-PSO And FB-K Means [14]	Fuzzy bisector K-means + Fractional PSO based neural network	78.00
A Fuzzy Clustering Approach Based On Multilayer Extreme Learning Machine For Brain Tumor Detection And Classification [35]	Fuzzy C Means clustering + Multilayer Extreme Learning Machine (ML-ELM)	95.00
Brain tumors detection and segmentation in MR images: Gabor wavelet vs. statistical features [09]	PCA with statistical features	79.30
Proposed	Quadtree Decomposition based fusion + GLCM + GLRLM+ ANN	93.97

V. CONCLUSION

Abnormal and uncontrolled growing of cells inside the brains leads to brain tumor. Usually treatment of these brain tumors depends on location and size of tumor. Although benign tumors do not tend to spread, but they may cause severe damage to brain by pressing its areas if not treated in early stage. Hence to avoid the manual errors an efficient automated intelligent classification technique is proposed. This work also involves an efficient fusion technique to fuse T1 and T2 MRI slices of brain, robust method like level set segmentation is also used to segment the tumor region, feature extraction methods like GLRLM and GLCM and ANN classifier for efficient detection and

REFERENCE

[1] Mohammad Havaei, Axel Davy, David Warde-Farley, Antoine Biard, Aaron Courville, Yoshua Bengio, Chris Pal, Pierre-Marc Jodoin and Hugo Larochelle, "Brain Tumor Segmentation with Deep Neural Networks", 2016.

[2] Bjoern H. Menze, Andras Jakab, Stefan Bauer, Jayashree Kalpathy-Cramer, Keyvan Farahani, Justin Kirby, Yuliya Burren, Nicole Porz, Johannes Slotboom, Roland Wiest, Levente Lanczi, Elizabeth Gerstner, Marc-André Weber, Tal Arbel, Brian B. Avants, Nicholas Ayache, Patricia Buendia, D. Louis Collins, Nicolas Cordier, Jason J. Corso, Antonio Criminisi, Tilak Das, Hervé Delingette, Çağatay Demiralp, Christopher R. Durst, Michel Dojat, Senan Doyle, Joana Festa, Florence Forbes, Ezequiel Geremia, Ben Glocker, Polina Golland, Xiaotao Guo, Andac Hamamci, Khan M. Iftekharuddin, Raj Jena, Nigel M. John, Ender Konukoglu, Danial Lashkari, José António Mariz, Raphael Meier, Sérgio Pereira, Doina Precup, Stephen J. Price, Tammy Riklin Raviv, Syed M. S. Reza, Michael Ryan, Duygu Sarikaya, Lawrence Schwartz, Hoo-Chang Shin, Jamie Shotton, Carlos A. Silva, Nuno Sousa, Nagesh K. Subbanna, Gabor Szekely, Thomas J. Taylor, Owen M. Thomas, Nicholas J. Tustison, Gozde Unal, Flor Vasseur, Max Wintermark, Dong Hye Ye, Liang Zhao, Binsheng Zhao, Darko Zikic, Marcel Prastawa, Mauricio Reyes and Koen Van Leemput, "The Multimodal Brain Tumor Image Segmentation Benchmark (BRATS)", IEEE, Vol. 34, Issue 10, 2015.

[3] Nelly Gordillo, Eduard Montseny and Pilar Sobrevilla, "State of the art Survey on MRI Brain Tumor Segmentation", Elsevier, Vol. 31, Issue 8, pp. 1426-1438, 2013.

[4] Xavier Llado, Arnau Oliver, Mariano Cabezas, Jordi Freixenet, Joan C. Vilanova, Ana Quiles, Laia Valls, Lluis Ramio-Torrenta and Àlex Rovira, " Segmentation of Multiple Sclerosis Lesions in Brain MRI: A Review of Automated Approaches", Elsevier, Vol. 186, pp. 164 – 185, 2012.

[5] M.H. Fazel Zarandi, M. Zarinbal and M. Izadi, "Systematic Image Processing for Diagnosing Brain Tumor S: A Type-II Fuzzy Expert System Approach", Elsevier, Vol. 11, 285–294, 2011.

[6] El-Sayed Ahmed El-Dahshan, Tamer Hosny and Abdel-Badeeh M. Salem, "Hybrid Intelligent Techniques for MRI Brain Images Classification", Elsevier, Vol. 20, pp. 433 – 441, 2010.

[7] T. Logeswari and M. Karnan, "An Improved Implementation of Brain Tumor Detection Using Segmentation Based on Hierarchical Self Organizing Map", International Journal of Computer Theory and Engineering, Vol. 2, No. 4, 2010.

[8] Kailash Sinha and G.R.Sinha, "Efficient Segmentation Methods for Tumor Detection in MRI Images", IEEE, pp. 1 – 6, 2014.

[9] Nooshin Nabizadeh and Miroslav Kubat, "Brain Tumor Detection and Segmentation in MR Images: Gabor Wavelet vs. Statistical Features", Elsevier, Vol. 45, pp. 286 – 301, 2015.

[10] Manavalan Radhakrishnan and Thangavel Kuttiannan, "Comparative Analysis of Feature Extraction Methods for the Classification of Prostate Cancer from TRUS Medical Images", IJCSI International Journal of Computer Science Issues, Vol. 9, Issue 1, Issue 2, 2012.

[11] Anam Mustaqeem, Ali Javed and Tehseen Fatima, "An Efficient Brain Tumor Detection Algorithm Using Watershed & Thresholding Based Segmentation", I.J. Image, Graphics and Signal Processing, Vol. 10, pp. 34 - 39, 2012.

[12] Wright, John, Yigang Peng, Yi Ma, Arvind Ganesh and Shankar Rao, "Robust Principal Component Analysis: Exact Recovery of Corrupted Low-Rank Matrices via Convex Optimization", Advances in Neural Information Processing Systems, 2009.

[13] Trinadh babu and Sk.Salma begum, "An Adaptive MRI Tumor Detection Using Neural Network Based Adaboost Algorithm", International Journal of Computer Science and Information Technologies, Vol. 6, Issue 1, pp. 42 - 47, 2015.

[14] Sheela.V.K and Dr. S. Suresh Babu, "Analysis and Evaluation of Brain Tumor Detection from MRI Using F-PSO and FB-K Means", International Journal of

Computer Science and Information Technology & Security (IJCSITS), Vol. 6, Issue 1, 2016.

[15] Mahantesh K and Kanyakumari, "BraTS: Brain Tumor Segmentation – Some Contemporary Approaches", International Journal of Innovative Research in Science, Vol. 5, Issue 10, 2016.

[16] Fazli Wahid, Muhammad Fayaz and Abdul Salam Shah, " An Evaluation of Automated Tumor Detection Techniques of Brain Magnetic Resonance Imaging (MRI)", International Journal of Bio-Science and Bio-Technology Vol. 8, Issue 2, pp. 265 – 278, 2016.

[17] Dr.A.R. Kavitha, L.Chitra and R.kanaga, "Brain Tumor Segmentation using Genetic Algorithm with SVM Classifier", International Journal of Advanced Research in Electrical, Electronics and Instrumentation Engineering, Vol. 5, Issue 3, 2016.

[18] Archana A.Mali and Prof.S.R.Pawar, "Detection & Classification of Brain Tumor", International Journal of Innovative Research in Computer and Communication Engineering, Vol. 4, Issue 1, 2016.

[19] Samriti and Mr. Paramveer Singh, "Brain Tumor Detection Using Image Segmentation", International Journal of Engineering Development and Research, Vol. 4, Issue 2, 2016.

[20] P.Senthil MA, "Image Mining Brain Tumor Detection using Tad Plane Volume Rendering from MRI (IBITA)", JOC, Vol. 1 Issue 1, pp. 1 - 13, 2016.

[21] G. Venkateswara Rao and O. Koteswara Rao, " Brain Tumor Detection and its Severity Analysis using Texture Features and Artificial Neural Network", International Journal of Advance Research in Computer Science and Management Studies, Vol. 4, Issue 5, pp. 174 – 182, 2016.

[22] Irfan Mehmood, Naveed Ejaz, Muhammad Sajjad and Sung Wook Baik, "Prioritization of Brain MRI Volumes using Medical Image Perception Model and Tumor Region Segmentation", Elsevier, Vol. 3, pp. 1471 – 1483, 2013.

[23] Leonardo Pacea, Emanuele Nicolaib, Angelo Luongoc, Marco Aiello, Onofrio A. Catalanob, Andrea Soricelli and Marco Salvatorec, "Comparison of Whole-Body PET/CT and PET/MRI in Breast Cancer Patients: Lesion Detection and Quantization of 18F-Deoxyglucose Uptake in Lesions and in Normal Organ Tissues", Elsevier, Vol. 83 pp. 289– 296, 2014.

[24] Khan M. Iftekharuddin, Jing Zheng, Mohammad A. Islam and Robert J. Ogg, "Fractal-Based Brain Tumor Detection in Multimodal MRI", Elsevier, Vol. 207, Issue 1, pp. 23 – 41, 2009.

[25] B. Hakyemez, C. Erdogan, G. Gokalp and A. Dusak, M. Parlak, "Solitary Metastases and High-Grade Gliomas: Radiological Differentiation by Morphometric Analysis and Perfusion-Weighted MRI", Elsevier, Vol. 65, pp. 15 – 20, 2010.

[26] Yongxin Zhang, Li Chen, Zhihua Zhao and Jian Jia, "Multi-focus Image Fusion Based on Sparse Features", International Journal of Signal Processing, Image Processing and Pattern Recognition Vol.7, Issue 2, pp. 399 – 410, 2014.

[27] Bing Nan Li, Chee Kong Chui, Stephen Chang and S.H. Ong, "Integrating Spatial Fuzzy Clustering with Level Set Methods for Automated Medical Image Segmenattion", Springer, Vol. 41, pp. 1-10, 2011.

[28] Aswini Kumar Mohanty, Swapnasikta Beberta and Saroj Kumar Lenka, "Classifying Benign and Malignant Mass using GLCM and GLRLM Based Texture Features from Mammogram", International Journal of Engineering Research and Applications (IJERA), Vol. 1, Issue 3, pp. 687 - 693, 2011.

[29] Eltaher Mohamed Hussein and Dalia Mahmoud Adam Mahmoud, "Brain Tumor Detection using Artificial Neural Networks", Journal of Science and Technology, Vol. 13, No. 2, 2012.

[30] N. Periyasamy and Dr. J. G. R. Sathiaseelan, "Detection and Classification of Brain Tumor Images Using Back Propagation Fuzzy Neural Network", International Journal for Research in Applied Science & Engineering Technology (IJRASET), Vol. 3, Issue VIII, 2015.

[31] Arashdeep Kaur , "An Automatic Brain Tumor Extraction System Using Different Segmentation Methods", IEEE, 2016.

[32] Imran Ahmed, Qazi Nida-Ur-Rehman, Ghulam Masood and Muhammad Nawaz, "Analysis of the Brain MRI for Tumor Detection & Segmentation", Proceedings of the World Congress on Engineering, Vol. I, 2016.

[33] Eman Abdel-Maksoud, Mohammed Elmogy and Rashid Al-Awadi, "Brain tumor segmentation based on a hybrid clustering technique", Egyptian Informatics Journal Vol. 16, pp. 71 – 81, 2015.

[34] Mohammad Havaeia, Axel Davyb, David Warde-Farleyc, Antoine Biardc,d, Aaron Courvillec, Yoshua Bengioc, Chris Palc,e, Pierre-Marc Jodoina and Hugo Larochellea, "Brain Tumor Segmentation with Deep Neural Networks", Medical image analysis, Vol. 35, pp. 18-31, 2016.

[35] M. Deepa and M. Rajalakshmi, "A Fuzzy Clustering Approach Based On Multilayer Extreme Learning Machine For Brain Tumor Detection and Classification", International Journal of Advanced Engineering Technology, Vol. VII, Issue I, pp. 896-902, 2016.

[36] El-Sayed Ahmed, El-Dahshan, Tamer Hosny, Abdel-Badeeh M. Salem, 'Hybrid intelligent techniques for MRI brain images classification', Elsevier, Vol. 20, pp. 433 - 441, 2010.